THE GEOLOGICAL SOCIETY OF AMERICA

Structural Controls of Hydrodynamic Anisotropy in the West Elk Mine Region, Western Colorado

RON HARRIS

ALLEN LUTHI

ALAN L. MAYO

Department of Geology, Brigham Young University, Provo, UT 84602

WENDELL KOONTZ

Mountain Coal Company, LLC, Somerset, CO 81434

Key Terms: ***Fault Architecture, Groundwater, Coal Mining, Structure, Colorado Plateau***

ABSTRACT

An investigation of the structure and hydrology of the West Elk Mine region reveals that variable local development of faults above an igneous cupola are parallel to systematic joints and *in situ* stresses, which in turn control groundwater storage and flow in the region. Six faults were found superimposed on a regional systematic joint set. Fault displacement and development decrease away from a magnetic anomaly interpreted as a pinnacle-shaped pluton. Measurements of displacement along the strike- and dip-lengths of faults reveal variations in shape, size, and structural architecture that correlate with the degree of fault zone development and structural complexity. A progression is found from single-fracture faults to more distributed, then more localized deformation, with increasing displacement toward the igneous intrusion.

Increasing rates of groundwater discharge also correlate with increasing fault displacement and development. Pump tests show immediate communication 50 m away from the most developed fault, but no response from the nearest neighboring fault (600 m away). The combined factors of very low matrix permeability ($<10^{-3}$ darcy), large groundwater storage volumes, variable and sometimes high groundwater discharge rates, and the absence of hydraulic communication between adjacent fault zones indicate the groundwater system is variably compartmentalized by differences in fault architecture.

INTRODUCTION

The structural architecture of faults can strongly influence fluid flow through rocks. For example, the core and damage zones of faults can act as both barriers to flow and conduits, depending on the degree of fault development and the connectivity and aperture of fractures (Chester and Logan, 1986; Smith et al., 1990; and Caine et al., 1996). Underground mines through faulted regions provide a way to document variations of fault architecture with fault development and how these variations may control groundwater storage and flow.

The West Elk Mine of southwest Colorado has experienced difficulties with water intrusion upon encountering fault zones (Figure 1). Rapid groundwater inflows (6 to 500 L/second) were measured from three separate faults during coal-mining operations. Even though the faults are only 600–1,000 m apart and are connected by a 100-m-thick laterally continuous sandstone unit, they are hydraulically isolated from one another (Mayo and Koontz, 2000). The combined factors of large groundwater storage volumes, variable and sometimes high groundwater inflow rates, and the absence of hydraulic communication between adjacent fault zones indicates that the structural architecture plays a significant role in the storage and movement of groundwater. Although fault-related groundwater discharge is common at both the surface and in underground openings, conceptual models of these compartmentalized flow systems are poorly constrained by direct observation and measurements.

In this article we present a structural analysis of fault and fracture systems that compartmentalize groundwater in the West Elk Mine region. Sub-surface mine workings provide rare access to fault and fracture systems as well as useful hydrodynamic data from horizontal and vertical drilling. Horizontal drilling between faults provides constraints on fault location and displacement, the thickness of damage and core zones, and the extent of hydrologic communication within and between faults. These data provide a way to explore how hydrodynamic anisotropy within the mine region may be explained by variation in structural architecture of fault zones. The structural analysis combines surface and sub-surface measurements to assess variation in shape, size, displacement, and archi-

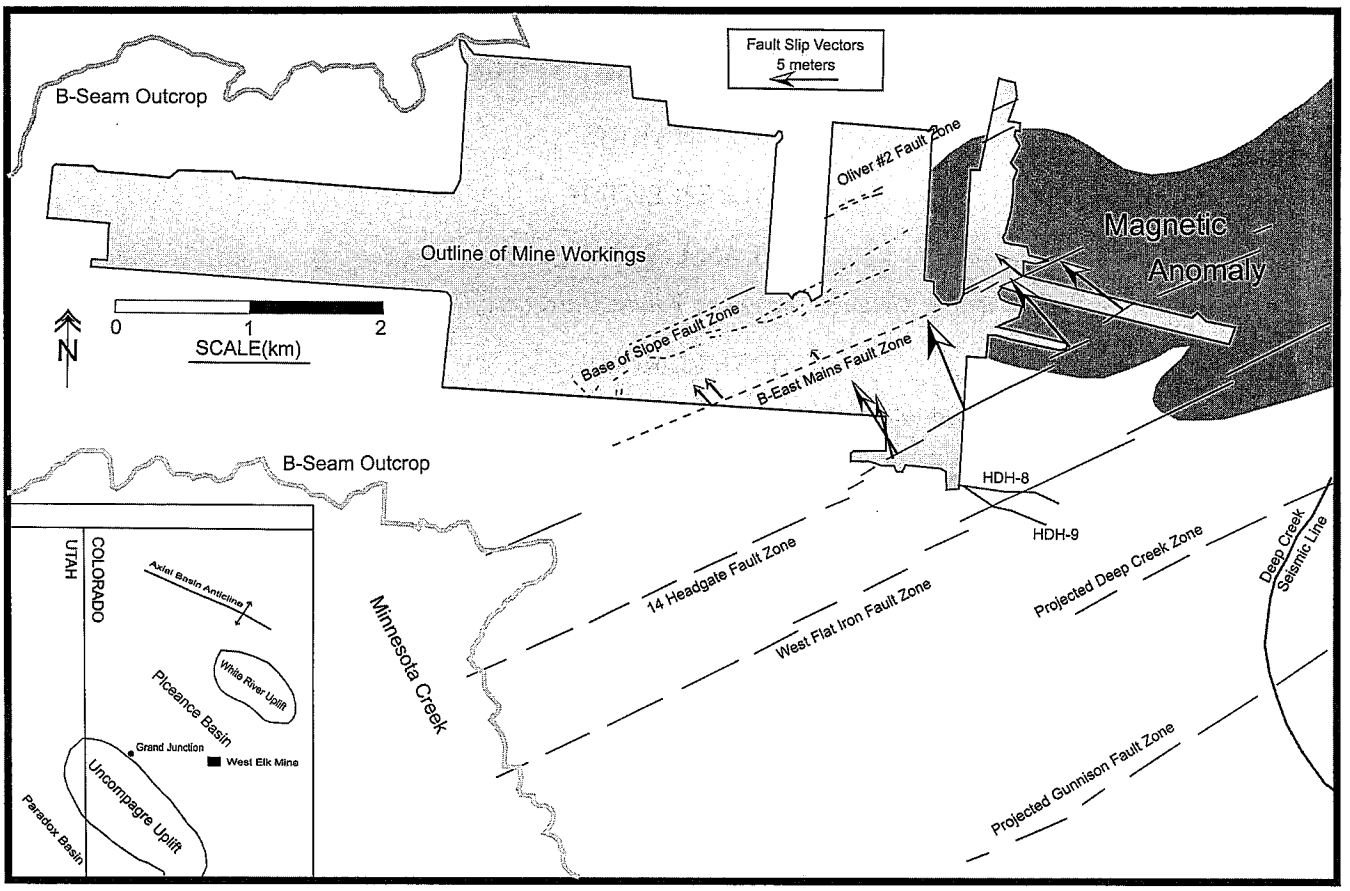

Figure 1. Map of the West Elk Mine region with a reference tectonic map of western Colorado. Light gray is underground mine workings of the B-seam. Dark gray is approximate area of magnetic anomaly, which may correspond to a cupola-shaped igneous intrusion at depth. Fault slip vector measurements show slight left-lateral component of extensional hanging-wall slip. Slip increases to a maximum in the 14 Headgate fault. All faults in the mine dip northwest.

tecture of faults and the age, chemistry, and transmissivity of groundwater in the fault zones.

GEOLOGIC SETTING

The stratigraphy of the West Elk Mine region consists mostly of clastic sedimentary units of the Tertiary Wasatch Formation, Cretaceous Mesa Verde Group, and Cretaceous Mancos Shale (Wellborn, 1982; Dunrud, 1989; and Van Wagoner et al., 1990, 1991). Only a few kilometers south and east of the mine area, a series of igneous laccoliths, sills, and dikes associated with the Oligocene Mount Gunnison porphyritic diorite intrude up through the Mancos Shale (Dunrud, 1989). Other plutons of unknown age are found a few kilometers to the north intruding up through much of the lower Mesa Verde Group coal-bearing units. These units include a 15- to 20-m-thick B-A-seam coal-bearing interval of the Lower Coal member and a 30- to 120-m-thick basal Rollins Sandstone Member. The Rollins Sandstone overlies the 1,200-m-thick Mancos Shale (Figure 2). In the West Elk Mine region, these units dip gently to the northwest away from the Mount Gunnison igneous intrusives.

Analysis of company aeromagnetic data indicate that a northeast-trending probable igneous cupola with north and south lobes intrudes up to about 1,500 to 3,000 m from the land surface beneath the eastern part of the mine (Figure 1). Based on the intensity of the magnetic anomaly, the pluton most likely reached the Mancos Shale. Although the intrusion has not greatly deformed the overlying sedimentary sequences, it has resulted in subtle structural effects visible in mine workings and may be responsible for significant topographic features at the surface. Broad flat mesas occur directly above the two lobes of the cupola, and valleys and steep slopes occur along the flanks. The Rollins Sandstone above the Mancos Shale has been gently domed above the lobes of the intrusion.

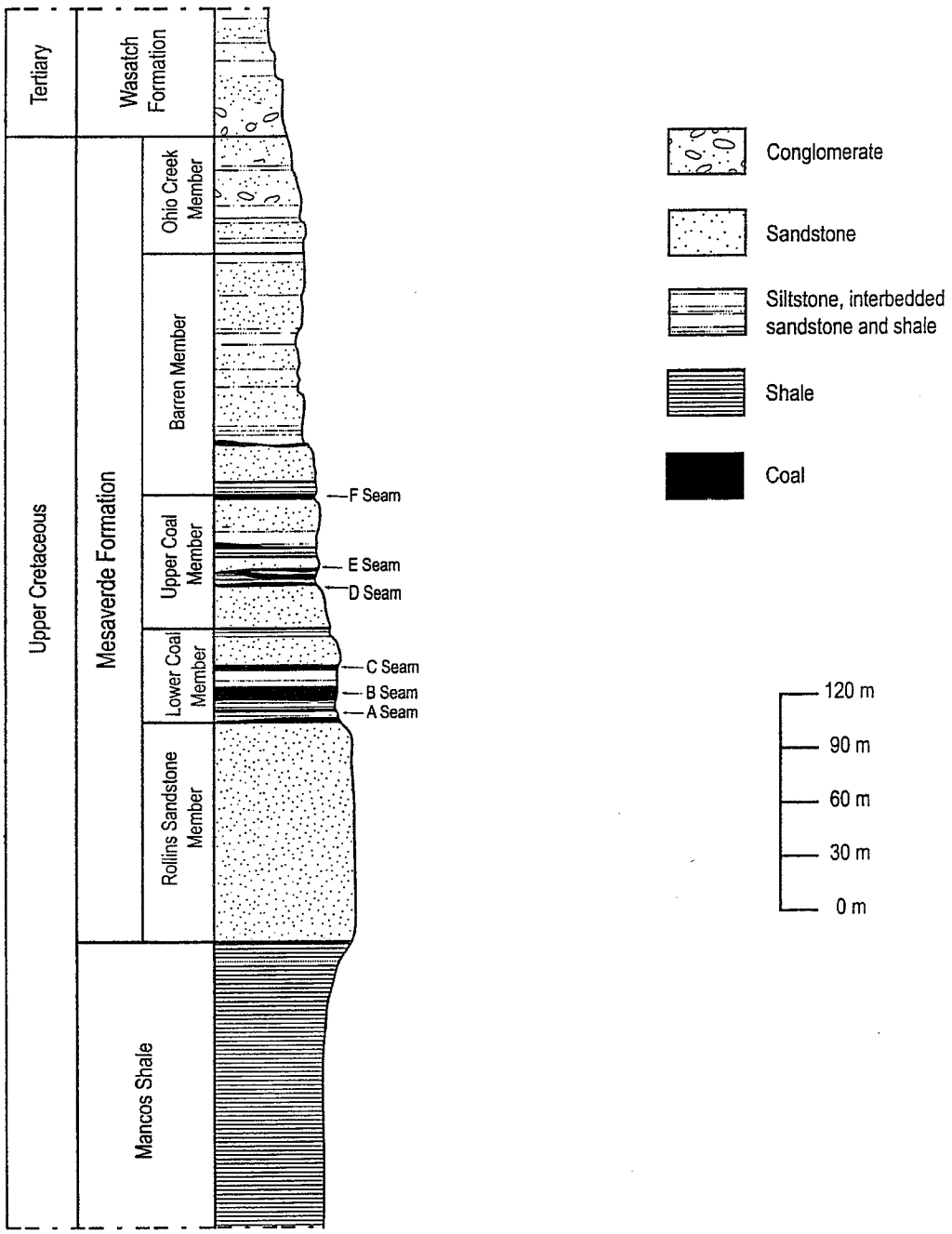

Figure 2. Stratigraphic column of strata near West Elk Mine from the Wasatch Formation to the Mancos Shale. The igneous intrusion is of unknown age and most likely penetrates much of the Mancos Shale (from Mayo and Koontz, 2000).

STRUCTURAL GEOLOGY

The structure of the mine is characterized in sequential order by differential compaction features, systematic and non-systematic joints, and mostly NE-SW–trending normal fault zones. Each of these structures is superimposed onto a northward-dipping, mechanically variable succession of sandstone, shale, and coal units, some of which are laterally discontinuous.

Joints

Bed-normal joints that terminate into bedding planes or pre-existing fractures are found throughout the Mesa Verde Group, but they are best expressed in sandstone units and as coal cleat. Two directions are present, a prevailing set of NE-SW–oriented systematic joints (J1) and a secondary set of curvy cross-joints (J2) that abut into J1 (Figure 3).

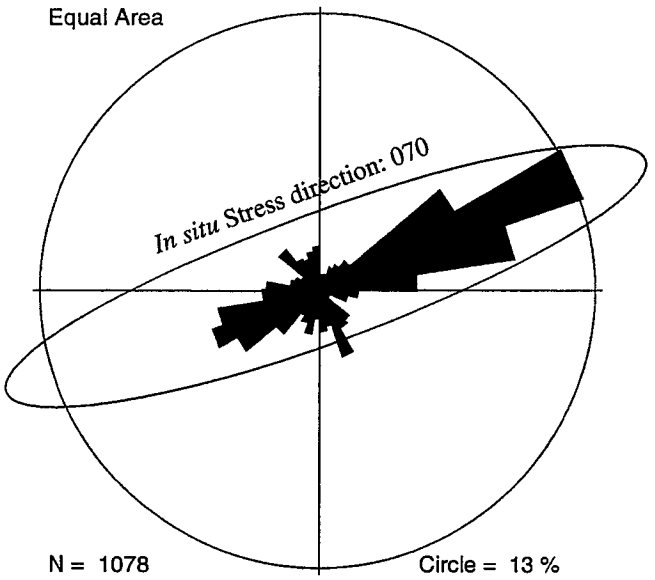

Figure 3. Rose diagram of joints measured in and near the West Elk Mine, including *in situ* stress ellipse. The stress ellipse major axis is 11.0 MPa, and the minor axis is 2.8 MPa (Maleki et al., 1996). Two separate sets of joints include a prevailing, systematic joint set and a subsidiary, non-systematic set. The strike projection is shown according to the right-hand rule, showing that the majority of the joints dip to the southeast.

The earliest joint set (J1) to form in the Mesa Verde Group is sub-parallel to the NE-SW–directed regional paleo-stress that produced the structural grain of southwest Colorado during Cretaceous and Early Tertiary time (Figure 1). The spacing of these joints is lithology controlled and varies mostly according to the thickness of individual sandstone units, producing a systematic pattern (Figure 4). Most joints are open, with apertures of one to a few millimeters. A stained zone surrounds most joints outcropping on the surface, attesting to the movement of fluids along the fractures. The cliff faces investigated in the surface study are mostly up-dip from the fault zones encountered in the mine, suggesting that the joints may serve as recharge pathways for aquifers at depth. J1 could also recharge strike-parallel, cross-cutting normal fault zones.

Non-systematic, curvy cross-joints are generally oriented NW-SE (Figure 3) and abut into and connect J1. Spacing of J2 is joint controlled and variable (1–10 m) because of the mechanical influence of pre-existing J1. J2 joints are not as long or abundant as those in J1 but may play an important role in fracture permeability by interconnecting J1.

Offsets of as much as 12 cm were discovered along closely spaced fracture sets at the tips of normal faults intersecting the Minnesota Creek cliff face (Figure 1). The sense of shear is consistently down to the northwest like that measured on fault planes within the mine. Fracture spacing decreases from around 3 m to 30–50 cm within the 3-m-wide zone adjacent to the offsets. Because minor slip occurred along closely spaced vertical fractures instead of along the inclined normal fault planes found throughout the mine, these fractures are interpreted as pinnate joints that form in front of the fault tip and comprise its damage zone.

Faults

Faults in the West Elk Mine region are localized above and on the flanks of the magnetic anomaly interpreted as an intrusive body and are not found in nearby mines or on the surface. Four oblique-slip normal faults have been encountered north of the anomaly by mine workings, and three normal faults south of the anomaly are inferred from seismic reflection profiles (Figure 1). The average spacing between the faults is around 1,000 m. The four faults within mine workings have slip surfaces that strike NE-SW and dip northwest at an average angle of 70° (Figure 5). Extensional displacement is generally away from the anomaly, with down-to-northwest slip north of the anomaly and down-to-southeast slip inferred from seismic lines south of the anomaly. Maximum displacements vary from 7.2 m along the 14 Headgate Fault (14 HG fault) to less than 0.5 m on the BC fault. Maximum displacements on other faults progressively decrease toward the northwest away from the anomaly (Figure 1).

The character of the faults also changes progressively from single-fault planes in the BC fault, to more diffuse distribution of displacement on the B-East Mains Fault (BEM fault) and the Base of Slope fault (BS fault), to localized deformation along the 14 HG fault. These differences in fault zone architecture can be explained as a progression through sequential steps in the growth of faults (Caine et al., 1996). As each fault experiences progressively more slip, it changes from a single-fault plane (BC fault), to a more diffuse zone of deformation (BEM fault), to a localized deformation zone (14 HG fault).

Fault architecture also varies with lithology. In coal seams there is a system of E-W–trending vertical faults with mostly horizontal slip surface features that increase in abundance toward the larger normal faults. The amount of displacement partitioning associated with these horizontal slip structures is ambiguous because of the lack of marker units. The presence of these structures is most likely a consequence of strain partitioning associated with the mechanical heterogeneity of the sedimentary sequence.

Fault Length and Displacement

Differences in fault architecture are also demonstrated by the variety of fault sizes and shapes, displacement

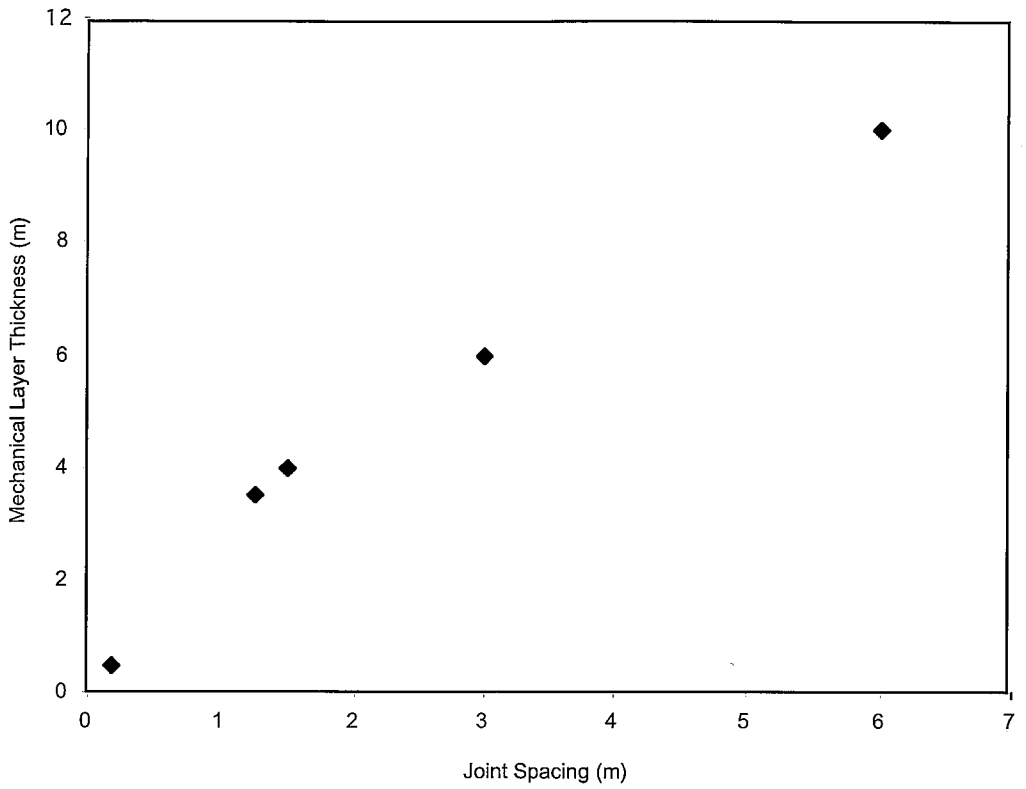

Figure 4. The relationship of joint spacing to mechanical layer thickness in the Minnesota Creek outcrops of the Rollins Sandstone member.

gradients, and relationships between displacement and gouge and damage zone thickness. None of the faults is expressed on the surface, which implies that they initiated at a greater depth than their dip-length. Because fault displacements generally decrease up-section from the Rollins Sandstone, it is likely that the faults initiated and maximum dip displacement occurs near the mechanical boundary between the Rollins Sandstone and underlying Mancos Shale.

Fault Dip Displacement Gradient

Fault dip displacement generally decreases with increased elevation, away from the Rollins Sandstone. The dip displacement gradient is the ratio of vertical displacement (throw) between two different parts of the fault. For example, if the B-Seam and F-Seam show the same amount of throw along a fault, the displacement gradient is 1:1. However, this is generally not the case. A displacement gradient of 5:3 is commonly observed along fault zones between the lower B-Seam and the higher F and E coal seams (Figure 6). These measurements at various stratigraphic intervals were obtained from mapping of different seams in the mine, drilling data, and magnetotelluric and seismic surveys.

Mining in both the B- and F-Seams allowed for direct measurements along the BS fault that reveal a maximum dip displacement gradient of 5:3. Drilling measurements were obtained from six vertical core holes that were drilled from the B- to the E-Seams, two along the 14 HG and BEM fault zones. Average dip displacement gradients are 5:3 for the 14 HG fault and 5:6 for the BEM fault.

Two horizontal drill tests to the southeast of the mine (HDH-8 and HDH-9) located the West Flat Iron fault zone (Figure 1). HDH-8 measured offset in the B-Seam, and HDH-9 was drilled up into and measured offset in the E-Seam. At this location, the dip displacement gradient along this fault is 5:3.

Magnetotelluric survey profiles were done across the 14 HG and BEM fault zones. The profile across the 14 HG fault shows an average dip displacement gradient of 3:2. The profile crossing the BEM fault has an average dip displacement of 4.8:5, which is close to the 5:6 gradient measured from drilling.

Measurements from seismic reflection data are limited by low resolution. However, the pattern of decreasing offset up-section is seen. The Deep Creek seismic line (Figure 7) does show more offset of the B-Seam than those higher in the section.

Analysis of dip displacement gradients obtained by these various methods suggest two different types of fault development. The majority of the fault systems show greater displacement lower in the section, with an

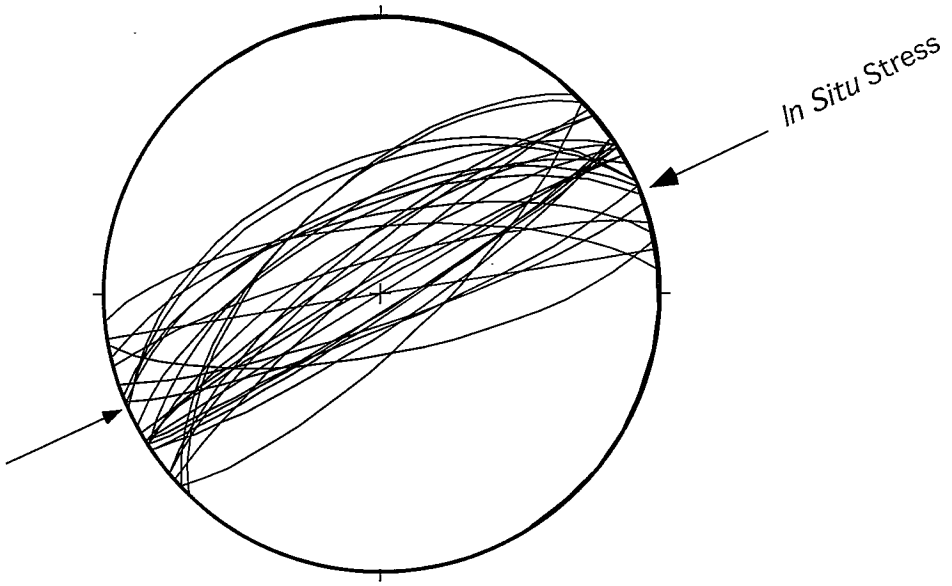

Figure 5. Equal-area stereograph of fault planes, which are sub-parallel to *in situ* stress directions. Most faults are steep and dip and slip down to the northwest.

average dip displacement gradient of around 5:3 from the B- to the overlying E- and F-Seams (Figure 6). This is most significant along the 14 HG fault, which shows the greatest displacement of any fault encountered within the mine. Faults exhibiting this type of displacement gradient likely initiated near, and have a maximum dip displacement at, the mechanical boundary between the Rollins Sandstone and underlying Mancos Shale. The BEM fault differs from this pattern. It yields average dip displacement gradients from two independent data acquisition methods of slightly greater displacements higher in the section.

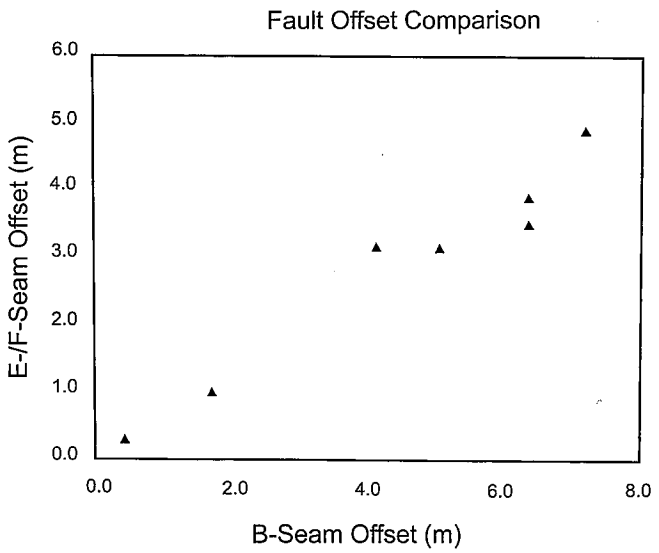

Figure 6. Vertical displacement comparison from the B-Seam to the E- and F-Seams. The dip displacement is greatest in the B-Seam and dies out up-section in all faults except the B-East Mains (BEM) Fault. These data imply that faults originated below the B-Seam, possibly in the Rollins Sandstone. The ratio of offset between the lower and upper seams is 5:3. In the BEM fault, there is no significant vertical displacement difference between the B- and E-Seams. This implies that faulting originated somewhere near the marine sandstone, between the two seams (Figure 2).

Fault Displacement Gradient along Strike

Displacement along the trend of the BEM and 14 HG faults decreases to less than a few centimeters toward the southwest over a distance of 4.5–5.0 km of strike-length where the damage zones of these faults intersect outcrops in Minnesota Creek (Figure 1). Although the overall strike-length is about the same for these faults, the patterns of displacement vary greatly (Figure 8). The BEM fault has a complex pattern (Figure 8A) more akin to distributed deformation along a series of *en echelon* fault segments with displacements down to the northwest of 0.6–2.5 m (Figure 1). Where displacement is transferred from one segment of the *en echelon* system to the other, the zone of distributed deformation widens.

In contrast, the displacement pattern for the 14 HG fault is characteristic of more localized deformation and produces a consistent ellipsoidal shape of strike-length versus displacement (Figure 8B). By assuming that the measured maximum displacements along the 14 HG fault occur at the half-strike-length of the fault, we estimate a total strike length of 4,500–5,000 m, which yields a displacement to strike-length ratio of 1:700–1:850. This ratio is in the under-slipped range of the

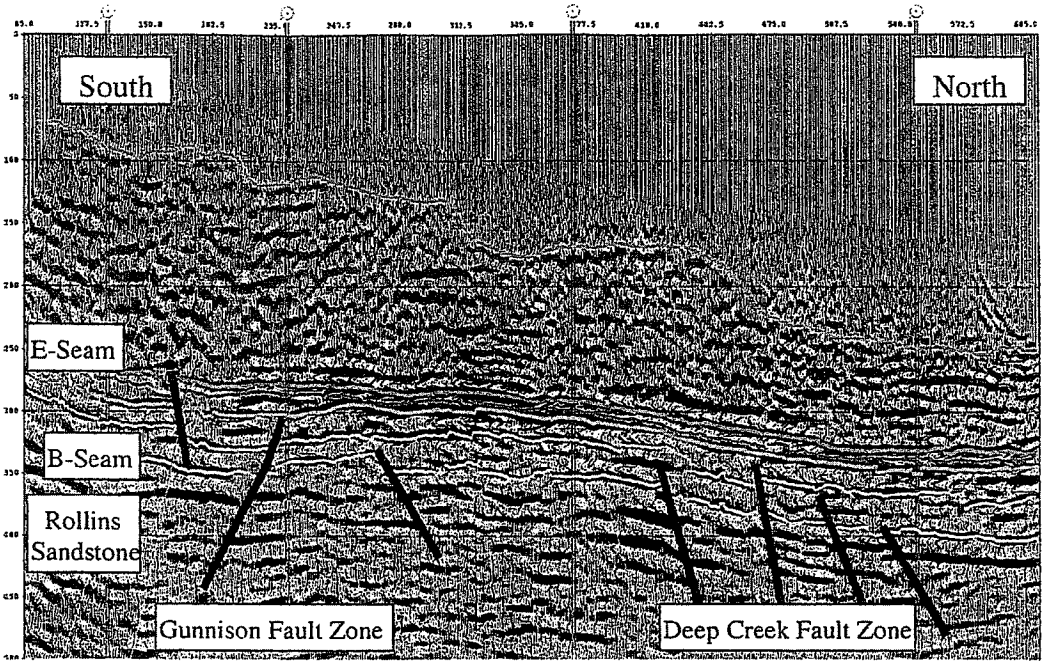

Figure 7. Deep Creek seismic line (see Figure 1 for approximate location). Note the degree of strain partitioning between stratigraphic horizons. In most cases fault displacement decreases up-dip from below the B-Seam, not offsetting the F-Seam. Some fault segments originate between the B- and F-Seams. Seismic line provided by Mountain Coal Company, LLC, and the West Elk Mine.

1:300–1:1,000 ratio predicted from studies of other faults (Muraoka and Kamata, 1983; Rippon, 1985; and Watterson, 1986). The missing slip may be accounted for by the evidence of slip partitioning observed in low strength units. The Deep Creek seismic line also shows strain partitioning between various units as well as from fault to fault (Figure 7).

Fault Slip Directions

Measurements of fault slip directions acquired from analysis of grooves on excavated fault planes show mostly dip slip, with up to 25 percent left-lateral oblique slip in places (Figure 1). The oblique-slip component may also explain the slightly low dip-slip values compared with fault length. The horizontal component of oblique-slip may be associated with the direction of pluton intrusion or the direction of topographic slope at the time of intrusion. The intrusion is most likely a finger of the larger Gunnison diorite body that lies to the south. Intrusion toward the northeast from the Gunnison body would impose a left-lateral sense of shear on normal faults oriented NE-SW. The paleo-maximum principal compressive stress ($\sigma 1$ in this situation) would plunge steeply to the southeast. The localized occurrence of oblique-slip normal faults in the region and the progressive decrease of maximum displacement on each fault to the northwest of the 14 HG Fault indicate that extensional deformation is most likely associated with local bending stresses or extensional collapse above the intrusion.

Damage Zones

Damage zones consisting of multiple fault planes, each of which is surrounded by a girth of closely spaced shear and tension fractures, are found on the three faults with the most displacement (Oliver 2, BEM, and 14 HG faults). Along the 14 HG fault, damage zone width varies with displacement and lithology. Where there is 6.4 m of displacement, the damage zone is at least 50 m thick in the Rollins Sandstone, compared with 14.8 m thick in the overlying coal layer. Fracture density in the damage zone is greater in the coal (2–5 cm apart) than in siltstone and sandstone units (3–10 cm apart). A strong correlation between gouge thickness and maximum displacement along faults supports the possibility that each fault is at a different developmental stage (Figure 9). These measurements are consistent with observations about faults summarized by Heynekamp and others (1999), which predict that faults:

1. Initiate in sand-rich and terminate in clay-rich beds
2. Widen in sand-rich beds because of cataclasis-induced strain hardening
3. Narrow in clay-rich beds because of strain softening caused by mechanical alignment of clays in the fault core

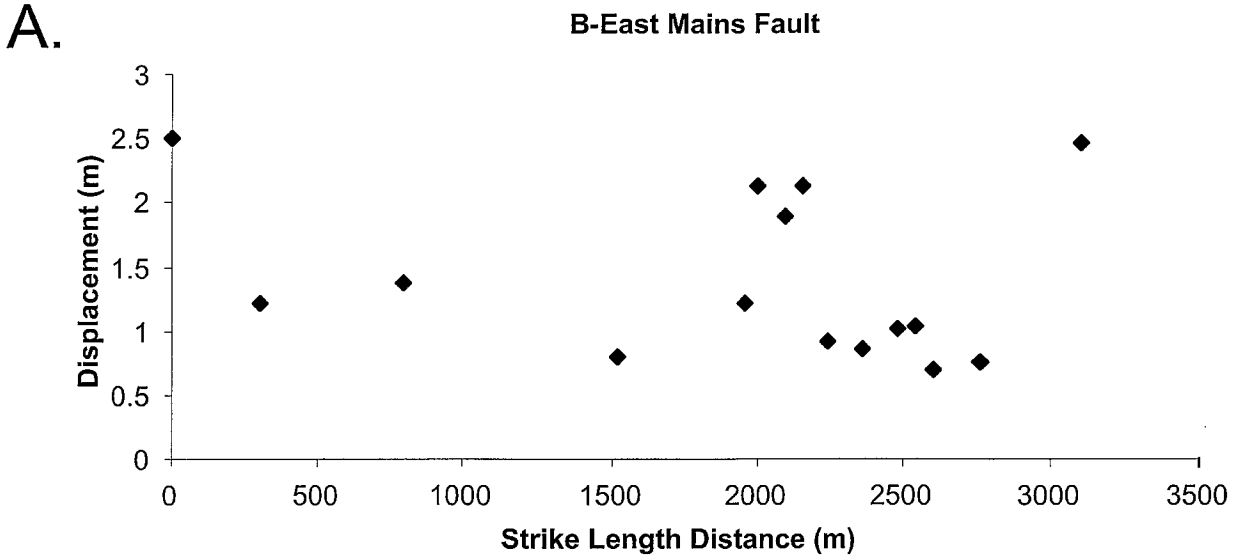

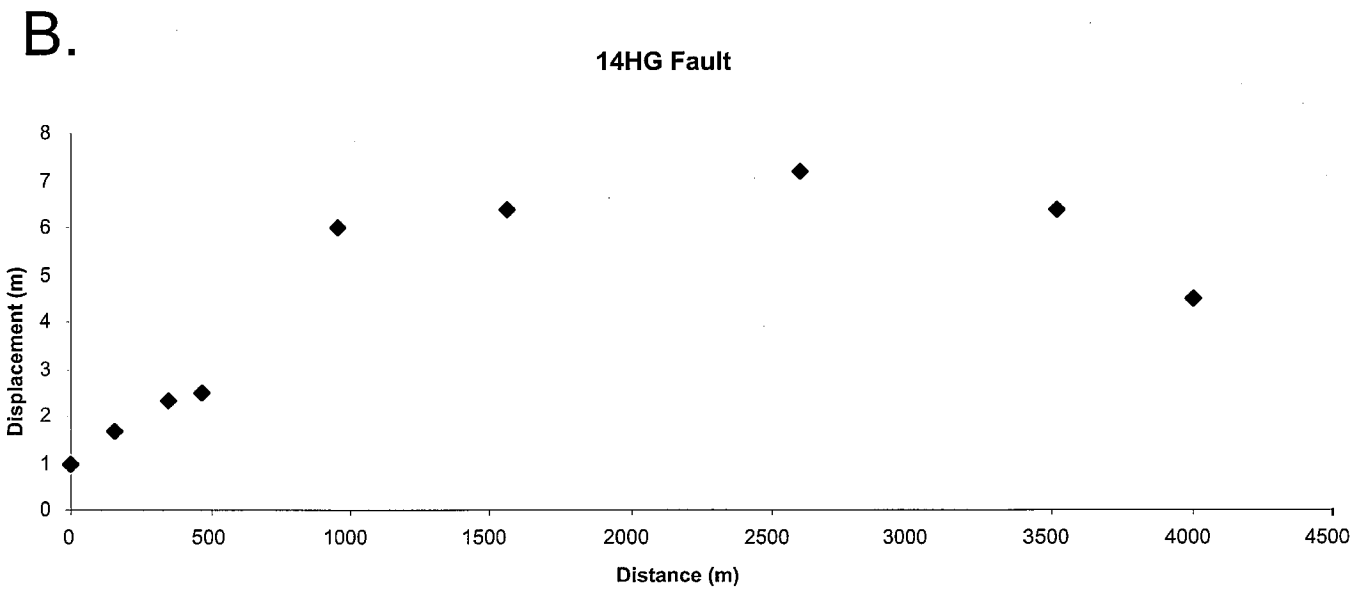

Figure 8. Plots of displacement versus strike length for (A) the B-East Mains (BEM) Fault and (B) the 14 Headgate (14 HG) Fault. The elliptical shape of the 14 HG fault versus the complex pattern of the BEM fault may be explained by the maturity of fault development, which is a function of strain localization versus partitioning.

GROUNDWATER SYSTEMS

Fault-Related Groundwater Discharge

Groundwater inflows into the mine environment occur only in association with faulted Rollins Sandstone, which is dry between faults. The magnitude of fault-related inflow from the Rollins Sandstone increased with southward mine development, which progressively encountered faults with greater amounts of maximum displacement and thicker damage zones (Figure 1). Mining into the BS fault yielded a flow of approximately 6 L/second of groundwater. Six years later, when mining encountered the BEM fault, an estimated 160 L/second issued from the mine floor, some 10 m above the top of the Rollins Sandstone. Eight months later the

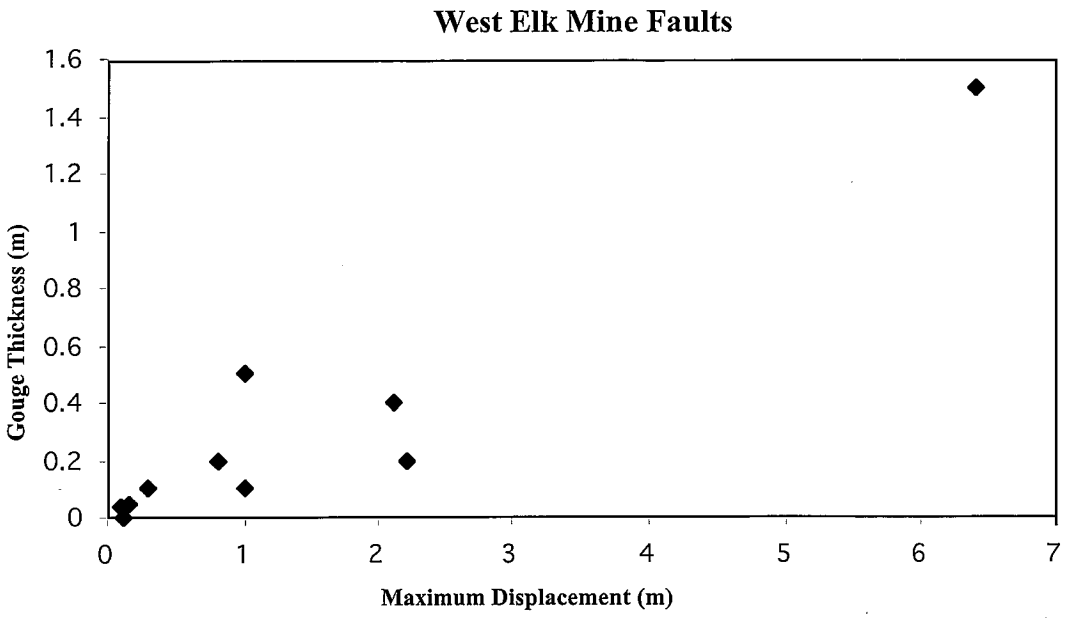

Figure 9. Comparison of fault gouge thickness to dip displacement shows that increased displacement increases fault core zone thickness.

mine penetrated the core of the 14 HG fault, striking the damage zone of the Rollins Sandstone footwall. Upon penetration of the fault, the mine floor catastrophically blew out and discharged 500 L/second of water, which flooded the mine. The discharge rate decreased with time and over a 2-year period achieved a total discharge of around 2.2×10^5 m^3.

By analysis of δ^2H and δ^{18}O compositions, ^{14}C ages as much as 10,500 years, and pump tests, Mayo and Koontz (2000) demonstrate that the groundwater in each fault system is hydraulically isolated. Matrix-permeability measurements on drill core from the Rollins Sandstone yield values of $<10^{-3}$ darcy (Mayo and Koontz, 2000). These low values are not nearly sufficient to have produced the total discharge from the 14 HG fault, which indicates that most, if not all, of the permeability is from fractures within the damage zones of faulted Rollins Sandstone.

Permeability within the damage zone of the 14 HG fault was evaluated by packer and constant head pumping tests. Vertical boreholes were used to pump wells, and inclined boreholes served as observation wells. The vertical borehole is located 50 m from the core zone of the 14 HG fault, and the inclined holes cross the fault. The pump test data show that a direct and immediate hydraulic communication exists between damage zone fractures in the Rollins Sandstone and the 14 HG fault for a minimum horizontal distance of 50 m (Mayo and Koontz, 2000). The full horizontal extent of this communication is unknown; however, the 14 HG fault system is not in hydraulic communication with the BEM fault system, about 670 m to the north of the test.

Except where broken by faulting, the low-permeability matrix of the Rollins Sandstone acts as a barrier to groundwater flow. Thin beds of carbonaceous shale and possibly other beds in the B- to A-Seam interval may also act as a significant seal that has helped prevent groundwater migration through fault-free zones in the Rollins Sandstone. These layers are confining units that have allowed the buildup of high artesian pressures.

Fracture-Controlled Transmissivity

Conceptual models of regional groundwater flow commonly assume that transmissivity is isotropic and controlled mostly by the gradient of the potentiometric surface. Yet, if hydrologic conductivity in the aquifer is fracture controlled, groundwater flow may be anisotropic, with transmissivities controlled mostly by the aperture and interconnectivity of fractures (Long and Witherspoon, 1985). These parameters in turn may be strongly influenced by *in situ* stresses (Brown and Bruhn, 1998) and the proximity to fault zones (Caine et al., 1996).

In the West Elk Mine region, the maximum *in situ* stress (σ1) is oriented 070°–080° (Maleki et al., 1996), which is within 10° of the mean orientation of J1 and most of the faults in the region (Figures 3 and 5). The aperture of these fractures in the mine is commonly as wide as 15 mm, with maximum widths of 17 cm in the blowout zone of the 14 HG fault. In outcrop, J1 fractures commonly have fluid alteration zones up to 20 cm thick, with up to 1.5 cm of poorly cemented sand along the fracture plane. In contrast, cross-joints, which are mostly oriented normal to σ1, have little to no aperture or fluid

staining. The dominance of fractures oriented NE-SW and the parallelism between these and $\sigma 1$ predispose the West Elk Mine region to anisotropic transmissivity.

CONCLUSION

Hydrodynamic anisotropy in the West Elk Mine was first suspected when very rapid inflows of groundwater occurred as fault zones were encountered during the mining operation. However, no faults related to far-field stresses are documented on the surface or in nearby mines. The outcrop and underground inspection of deformation features conducted here indicates that this hydrodynamic anisotropy may be attributed to the superposition of local extensional deformation above an intrusive body onto a pre-existing regional systematic joint set.

The Rollins Sandstone is broken by a systematic set of joints oriented parallel to NE-SW regional paleostresses responsible for much of the structural grain of western Colorado. Superimposed on the systematic joint set is a system of joint-parallel oblique-slip normal faults. The faults show a progressive decrease in structural complexity away from a magnetic anomaly interpreted as a cupola-shaped igneous intrusion. The fault nearest the anomaly (14 HG fault) has developed a localized deformation style with an extensive damage zone capable of discharging 500 L/second from a narrow opening created during mining near the fault core.

The groundwater system is highly compartmentalized by deformation features associated with each fault and low matrix permeability in the Rollins Sandstone and other units of the coal-bearing succession. A pump test confirmed that fractures in the damage zone are open enough and well enough connected to allow immediate communication over a minimum distance of 50 m away from the fault core. However, no response was detected on neighboring faults no more than 600 m away.

Other factors contributing to hydrodynamic anisotropy in the mine are the degree of fault zone development, parallelism of systematic joints and fault zones with maximum *in situ* stress direction, and mechanical and hydrodynamic heterogeneity of the coal-bearing succession. These factors cause variations in (1) the size and shapes of faults, (2) the width of damage zones, (3) fracture density, and (4) fracture aperture, which are the major controlling factors of hydraulic conductivity in rocks with low matrix permeability.

REFERENCES

BROWN, S. R. AND BRUHN, R. L., 1998, Fluid permeability of deformable fracture networks: *Journal Geophysical Research, B, Solid Earth Planets,* Vol. 103, No. 2, pp. 2489–2500.

CAINE, S. C.; EVANS, J. P.; AND FORSTER, C. B., 1996, Fault zone architecture and permeability structure: *Geology,* Vol. 24, No. 11, pp. 1025–1028.

CAINE, J. S., AND FORSTER, C. B., 1999, Fault zone architecture and fluid flow: Insights from field data and numerical modeling. In Haneberg, W. C.; Mozley, P. S.; Moore, J. C.; and Goodwin, L. B. (Editors), *Faults and Subsurface Fluid Flow in the Shallow Crust,* Geophysical Monograph 113, pp. 101–127.

CHESTER, F. M. AND LOGAN, J. M., 1986, Implications for mechanical properties of brittle faults from observations of the Punchbowl fault zone. In Wang, C. (Editor), *International Structure of Fault Zones: Pure and Applied Geophysics,* Vol. 124, No. 1–2, pp. 79–106.

DUNRUD, R. C., 1989, *Geologic Map and Coal Stratigraphic Framework of the Paonia Area, Delta and Gunnison Counties, Colorado:* U.S. Geological Survey, Coal Investigations Map C-115.

HEYNEKAMP, M. R.; GOODWIN, L. B.; MOZLEY, P. S.; AND HANEBERG, W. C., 1999, Controls on fault-zone architecture in poorly lithified sediments, Rio Grande Rift, New Mexico: Implications for fault-zone permeability and fluid flow. In Haneberg, W. C.; Mozley, P. S.; Moore, J. C.; and Goodwin, L. B. (Editors), *Faults and Subsurface Fluid Flow in the Shallow Crust,* Geophysical Monograph 113, pp. 27–50.

LONG, J. C. S. AND WITHERSPOON, P. A., 1985, The relationship of the degree of interconnection to permeability in fracture networks: *Journal Geophysical Research, B,* Vol. 90, No. 4, pp. 3087–3098.

MALEKI, H.; CLANTON, J.; KOONTZ, W.; AND PAPP, A., 1996, *The Relationship between Far-Field Horizontal Stress and Geologic Structure,* Report for the West Elk Mine, Colorado.

MAYO, A. AND KOONTZ, W., 2000, Fracture flow and groundwater compartmentalization in the Rollins Sandstone, Lower Mesaverde Group, Colorado, USA: *Hydrogeology Journal,* Vol. 8, No. 4, pp. 430–446.

MURAOKA, H. AND KAMATA, H., 1983. Displacement distribution along minor fault traces: *Journal Structural Geology,* Vol. 5, pp. 483–495.

RIPPON, J. H., 1985, Contoured patterns of the throw and hade of normal faults in the coal measures (Westphalian) of north-east Derbyshire: *Proceedings Yorkshire Geological Society,* Vol. 45, No. 3, pp. 147–171.

SMITH, L.; FORSTER, C. B.; AND EVANS, J. P., 1990, Interaction of fault zones, fluid flow, and heat transfer at the basin scale. In *Hydrogeology of Permeability Environments: International Association of Hydrogeologists,* Vol. 2, pp. 41–67.

VAN WAGONER, J. C.; JONES, C. R.; TAYLOR, D. R.; NUMMEDAL, D.; JENNETTE, D. C.; AND RILEY, G. W., 1991, Sequence stratigraphic applications to shelf sandstone reservoirs: Outcrop subsurface examples, in *American Association Petroleum Geologists, Field Conference Guidebook.*

VAN WAGONER, J. C.; MITCHUM, R. M.; CAMPION, K. M.; AND RAHMANIAN, V. D., 1990, Siliciclastic sequence stratigraphy in well logs, cores, and outcrops: Concepts for high-resolution correlation of time and facies: *AAPG Methods in Exploration Series 7.*

WATTERSON, J., 1986, Fault dimensions, displacements and growth. In Wang, C. (Editor), *International Structure of Fault Zones: Pure and Applied Geophysics,* Vol. 124, No. 1–2, pp. 365–373.

WELLBORN, J. E. F., 1982, *Stratigraphy of the Mesa Verde Formation, Mount Gunnison Coal Property, Gunnison County, Colorado:* Unpublished Master's Thesis, Colorado School of Mines, Golden, CO.